

Markovian Scale Prediction: A New Era of Visual Autoregressive Generation

Yu Zhang¹ Jingyi Liu¹ Yiwei Shi² Qi Zhang¹ Duoqian Miao^{1*}
Changwei Wang¹ Longbing Cao³

¹Tongji University ²University of Bristol ³Macquarie University

Project Page: <https://luokairo.github.io/markov-var-page/>



Figure 1. Visualization of generated images from our Markov-VAR at 256×256 or 512×512 on ImageNet benchmark.

Abstract

Visual AutoRegressive modeling (VAR) based on next-scale prediction has revitalized autoregressive visual generation. Although its full-context dependency, i.e., modeling all previous scales for next-scale prediction, facilitates more stable and comprehensive representation learning by leveraging complete information flow, the resulting computational inefficiency and substantial overhead severely hinder VAR’s practicality and scalability. This motivates us to develop a new VAR model with better performance and efficiency without full-context dependency. To address this, we reformulate VAR as a non-full-context Markov process, proposing Markov-VAR. It is achieved via Markovian Scale Pre-

diction: we treat each scale as a Markov state and introduce a sliding window that compresses certain previous scales into a compact history vector to compensate for historical information loss owing to non-full-context dependency. Integrating the history vector with the Markov state yields a representative dynamic state that evolves under a Markov process. Extensive experiments demonstrate that Markov-VAR is extremely simple yet highly effective: Compared to VAR on ImageNet, Markov-VAR reduces FID by 10.5% (256×256) and decreases peak memory consumption by 83.8% (1024×1024). We believe that Markov-VAR can serve as a foundation for future research on visual autoregressive generation and other downstream tasks.

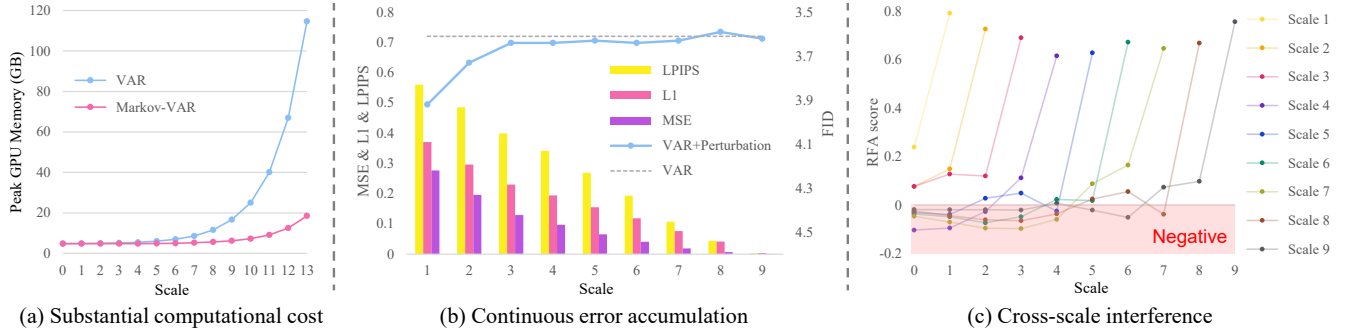


Figure 2. Observations of the challenges caused by full-context dependency. (a) Comparison of peak computation state (Activations + KV Cache) memory consumption between depth-24 VAR and Markov-VAR on generating 1024×1024 images with a batch size of 25. (b) Metrics and FID performance of VAR under perturbations injected at different scales. MSE, L1 and LPIPS jointly decrease as the perturbation injection scale shifts larger, indicating that early injected perturbations cause greater performance degradation. This is also evidenced by VAR’s largest FID drop at the first injection scale. (c) Residual-Feature Alignment scores (RFA) between each scale and its every previous scale. It is calculated as the cosine similarity between the output residual feature of the current scale and each input feature of all previous scales, combined with 1×1 convolution projection and square root operation, and preserves the directional contribution.

1. Introduction

As a general modeling paradigm, autoregressive modeling has dominated text generation [1, 7, 55, 59, 60] and multimodal understanding [6, 27, 64]. Yet, due to suboptimal generation quality, it was not widely adopted in visual generation tasks for a long time. Recently, Visual AutoRegressive modeling (VAR) [52] converts next-token prediction to next-scale prediction, further unleashing the potential of the autoregressive modeling to generate high-quality visual content, making autoregression once again a mainstream modeling paradigm for visual generation [17, 24, 41, 46]. However, VAR’s full-context dependency, requiring attention over all previous scales for next-scale prediction, can introduce certain challenges in practice:

I. Substantial computational cost. As the scale increases, the number of tokens grows quadratically. Moreover, cumulative modeling across multiple previous scales in VAR accelerates the superlinear increase in computational cost, as shown in Figure 2 (a). Such substantial computational cost not only slows down training and inference, but also severely limits VAR’s scalability and practicality.

II. Continuous error accumulation. As a chain-based modeling paradigm, autoregression’s unidirectional causality chain prevents early prediction errors from being corrected and leads to their continuous propagation. Figure 2 (b) shows that early perturbations impact the performance more severely than late ones, indicating that errors continuously accumulate during error propagation. In addition, VAR exacerbates the error accumulation in two aspects. First, its full-context dependency repeatedly utilizes and iteratively accumulates errors from previous scales. Second, rapid growth of the token sequence length extends the chain of error propagation and accumulation. This cross-scale er-

ror accumulation significantly degrades both the quality and stability, especially for high-resolution visual generation.

III. Cross-scale interference. VAR’s coarse-to-fine modeling requires learning distinctive scale-specific representations at each scale. However, for the current scale, full-context dependency leads attention to aggregate all previous scales, where mixed information of multiple scales makes attention and gradients from different scales compete or conflict with each other in the shared feature space, thereby suppressing the learning of distinctive representations at the current scale and limiting the improvement of generation quality. As illustrated in Figure 2 (c), we compute RFA scores to quantify the directional contribution of the input feature from previous scales to the current predicted residual feature, further measuring cross-scale consistency in learning the current representation. We find that early scales typically have a negative impact on learning distinctive representations at the current scale.

These challenges motivate us to explore *whether it is feasible to develop a visual autoregressive generation model without full-context dependency that outperforms traditional VAR in both performance and efficiency*. Inspired by the concept of sufficient statistics [2, 53, 54] in information theory, we suppose that each node in continuous chain-based propagation inherently maintains historical information to a certain extent. Appropriately distilling this into a representative dynamic state can achieve effective prediction without relying on all original historical information.

In light of this motivation, we develop Markov-VAR, a visual autoregressive generation model with Markov process. Markov-VAR refines next-scale prediction into **Markovian scale prediction**, where each scale prediction depends only on the current one rather than all previous scales. Chain-based unidirectional autoregressive model-

ing makes the current scale already encoding representative historical information for feature prediction [34, 62, 66]. Thus, we can treat each scale as a Markov state. However, non-full-context dependency inevitably discards substantial original historical information compared to full-context dependency. We establish a lightweight history compensation mechanism to enrich the Markov state for historical information. Specifically, we employ a sliding window that compresses certain previous scales within it into a compact history vector, which is then integrated with the Markov state to construct a representative dynamic state. By modeling these dynamic states as a Markov process, Markov-VAR achieves Markovian scale prediction.

Extensive experiments demonstrate Markov-VAR’s superior performance and efficiency. For image generation on ImageNet [9], compared to VAR, Markov-VAR reduces FID from 3.61 to 3.23 (256×256) and remarkably decreases peak memory consumption of the computation state from 117.9GB to 19.1GB (1024×1024). As a foundation model, its performance and efficiency may become more promising when combined with other enhancement or acceleration techniques. Moreover, Markov-VAR outperforms many alternative-paradigm models or improved VAR-like variants in various comparisons. Our contributions are as follows:

- We advance visual autoregressive generation by exploring modeling without full-context dependency, refining next-scale prediction as Markovian scale prediction to reformulate VAR as a non-full-context Markov process.
- We propose Markov-VAR with a history compensation mechanism to mitigate the historical information loss in the Markov process. Markov-VAR comprehensively surpasses VAR in both performance and efficiency, extremely simple yet highly effective.
- We publicly release the full series of Markov-VAR model weights, hoping to serve as a foundation model and facilitate future research on various tasks.

2. Related Work

Visual Autoregressive Generation. Early visual autoregressive generation models such as PixelRNN [57], PixelCNN [56] and PixelCNN++ [43] achieved pixel-level conditional modeling, yet this paradigm suffers from limited long dependency and extremely slow sampling. Subsequent works [11, 12, 26, 40, 58, 69, 73] treating image synthesis as a token prediction task relied on Vector Quantization (VQ) [58] to discretize continuous feature maps and autoregressively modeling visual token sequence. However, their raster-scan prediction order conflicts with the spatial structure of the images, leading to inferior performance compared to other alternative-paradigm models [14, 16, 18, 19, 23, 47, 48]. Recently, VAR [52] reformulates next-token prediction as next-scale prediction, further improving the generation quality of visual content. Some VAR-like vari-

ants, such as Infinity [17], HART [51] and VAR-CLIP [70] extend VAR to text-to-image generation. Other further improved VAR-like models [15, 21, 30, 31, 39, 63, 65, 74] perform various tasks, such as image super-resolution [38], 3D Object Generation [5] and image editing [61].

Chain-based Markov Modeling. The Markov assumption [35] that posits that the current state depends only on its immediate predecessor, has been widely employed for research in deep learning. Diffusion-based models [8, 36, 71, 72] have achieved remarkable success in various tasks based on this principle. As autoregressive models evolved to involving extremely long sequences, chain-based Markov modeling has been introduced to alleviate the challenges of long-context modeling. MARCOS [32] and MCoT [67] introduce structured memory nodes that reformulate chain-of-thought reasoning into a Markovian process for more lightweight inference. In visual autoregressive modeling, although HMAR [24] pioneeringly introduces Markov dependency to enhance generation performance, it comes at the cost of increasing the number of inference steps and the token sequence length. In this paper, we revisit this challenging trade-off problem and employ chain-based Markov modeling to develop a visual autoregressive foundation model that reconciles performance with efficiency.

3. Method

3.1. Preliminary: Next-Scale Prediction

VAR [52] reformulates autoregressive modeling from next-token prediction to next-scale residual feature prediction, which generates images in a coarse-to-fine manner based on full-context dependency. The modeling process involves T multi-scale residual features $\{R_1, R_2, \dots, R_T\}$ defined by a size set $\{S_1 \times S_1, S_2 \times S_2, \dots, S_T \times S_T\}$. At the t -th scale, VAR predicts the residual feature $R_t \in \mathbb{R}^{S_t \times S_t}$ based on all previous residual scales $R_{<t} = \{R_1, R_2, \dots, R_{t-1}\}$. The autoregressive likelihood is formulated as follow:

$$p(R_1, R_2, \dots, R_T) = \prod_{t=1}^T p(R_t \mid \langle \text{sos} \rangle, R_{<t}), \quad (1)$$

where $R_{<t}$ denotes the “prefix” of R_t , and $\langle \text{sos} \rangle$ is the start conditional embedding.

3.2. Markovian Scale Prediction

In contrast to VAR, Markov-VAR is based on Markovian scale prediction. The prediction process treats each scale as a Markov state and models it as a chain-based Markov process. The size set $\{S_1 \times S_1, S_2 \times S_2, \dots, S_T \times S_T\}$ defines T multi-scale residual features $\{R_1, R_2, \dots, R_T\}$. At the t -th scale, Markov-VAR predicts the Markov state $M_t \in \mathbb{R}^{S_t \times S_t}$ based on the Markov state M_{t-1} (the current

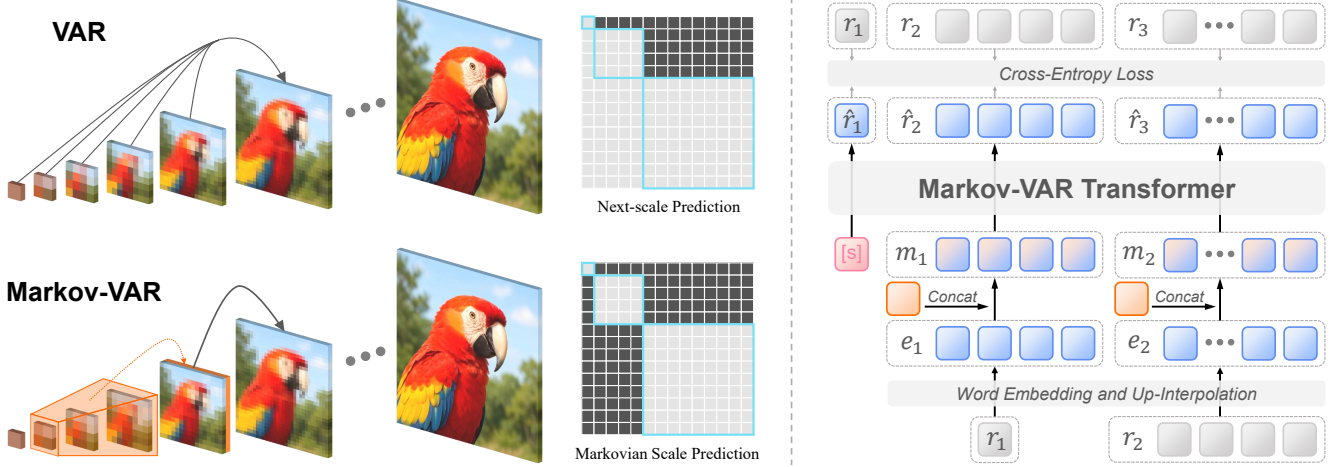


Figure 3. Left: Comparison of modeling process between VAR and Markov-VAR when predicting the 6-th scale & Comparison of visual context between next-scale prediction and Markovian scale prediction during generation. Markov-VAR utilizes a **history compensation mechanism** to enrich the current scale for historical information. Right: The overall framework of Markovian scale prediction with Markov-VAR Transformer. [S] is the start token with condition embedding.

residual feature R_{t-1}). Therefore, Markovian autoregressive likelihood can be formulated as follows:

$$p(R_1, R_2, \dots, R_T) = \prod_{t=1}^T p(R_t | M_{t-1}), \quad (2)$$

where Markovian state $M_t = f_\phi(R_t, M_{t-1})$ is a representative dynamic state for the residual feature R_t , and $f_\phi(\cdot)$ is a state update function, $M_0 = \langle \text{sos} \rangle$.

3.3. Markov-VAR

Figure 3 illustrates the comparison between VAR and Markov-VAR, and more details of Markov-VAR.

Markov State. Classical information theory [54] and its applications in deep learning [2, 53] indicate that: information $I(c_{<t}; c_t)$ of the complete history $c_{<t}$ with the current time c_t is highly redundant. There exists a sufficient statistic c_{t-1} such that: $I(c_{t-1}; c_t) = I(c_{<t}; c_t)$. Therefore, we argue that continuous chain-based modeling can propagate this sufficient statistic, enabling effective prediction of subsequent scales only based on the current scale. This theory allows us to naturally treat each scale as a Markov state.

History Compensation Mechanism. While each scale can be directly treated as a Markov state and modeled in a Markov process, it must be acknowledged that Markovian scale prediction performs suboptimally compared to next-scale prediction based on full-context dependency when the current scale cannot possess the complete sufficient statistic or substantial historical information is discarded. To maintain the Markov process while further improving prediction

performance, we design a history compensation mechanism to supplement historical information for prediction.

We set a sliding window \mathcal{W} of size N to store the previous N continuous scales. For the t -th residual scale R_t , the corresponding sliding window \mathcal{W}_t is denoted as:

$$\mathcal{W}_t = \{E_{t-1}, E_{t-2}, \dots, E_{t-N}\}, \quad (3)$$

where $E_t \in \mathbb{R}^{n^t \times d}$ denotes the embedded feature at the t -th scale, which is obtained through word embedding and up-interpolation of the residual scale R_{t-1} . n^t is the number of tokens at the t -th scale and d is the dimension of token.

We define the token sequence of E_t as $X_t \in \mathbb{R}^{n^t \times d}$. Thus, the overall token sequence \hat{X}_t of all scales within the sliding window is obtained by a concat operation: $\hat{X}_t = \text{Concat}(X_{t-1}, X_{t-2}, \dots, X_{t-N})$. We aggregate \hat{X}_t into a fixed-dimensional history vector h_t via cross-attention:

$$h_{t-1} = \text{Attn}(q, \hat{X}_t, \hat{X}_t), \quad (4)$$

where q is a learnable query representing the global state, and \hat{X}_t provides the key-value pairs.

When predicting the t -th residual scale R_t , we broadcast the history vector h_{t-1} : $H_{t-1} = \mathbf{1}_{n_{t-1}} h_{t-1}^\top$, and concatenate history vectors H_{t-1} and feature scale E_{t-1} element-wise to obtain a representative dynamic state M_{t-1} :

$$M_{t-1} = \text{Concat}(E_{t-1}, H_{t-1}). \quad (5)$$

After modeling the evolution of representative dynamic states as a Markov process, Markov-VAR starts to operate.

3.4. Training Strategy

Following the conventional autoregressive paradigm, we construct the ground-truth residual feature sequence R

Algorithm 1: Training Process of Markov-VAR

Input: $[R_1, \dots, R_T], N, (S_t \times S_t)_{t=1}^T$
Output: Trained model parameters θ
 $M = [M_0, \dots, M_{T-1}], M_0 \leftarrow \langle \text{sos} \rangle;$
 $\mathcal{F} \leftarrow \text{Queue}(); \mathcal{W} \leftarrow \text{Queue}();$
 $\text{Queue_Push}(\mathcal{F}, \langle \text{sos} \rangle); \hat{f} \leftarrow \text{tensor}(0);$
forall $t = 1$ **to** $T - 1$ **do**
 $\hat{f} = \hat{f} + \text{Up}(R_t, S_t); \quad // \triangleright \text{Add residual}$
 $E_t = \text{Embed}_\theta(\text{Down}(\hat{f}, S_{t+1}));$
 $\text{Queue_Push}(\mathcal{F}, E_t)$
end
forall $t = 1$ **to** $T - 1$ **do**
 if $\mathcal{W}.size() == N$ **then**
 $\text{Queue_Pop}(\mathcal{W}); \quad // \triangleright \text{Slide window}$
 end
 $X_t = \text{Queue_Front}(\mathcal{F});$
 $\text{Queue_Pop}(\mathcal{F});$
 $\text{Queue_Push}(\mathcal{W}, X_t); \quad // \triangleright \text{Slide window}$
 $\hat{X}_t = \text{Concat}(\mathcal{W});$
 $H_t = \text{Broadcast}(\text{Attn}(q_\theta, \hat{X}_t, \hat{X}_t));$
 $M_t = \text{Concat}(\mathcal{F}.Front(), H_t); \quad // \triangleright \text{Update}$
end
 $[\hat{R}_1, \dots, \hat{R}_T] \leftarrow \text{Model}_\theta([M_0, \dots, M_{T-1}]);$
 $\mathcal{L} = \sum_{t=1}^T \text{CE}(\hat{R}_t, R_t); \quad // \triangleright \text{Compute loss}$
 $\mathcal{L}.Backward(); \quad // \triangleright \text{Update } \theta \text{ via } \mathcal{L}$
return θ

as the supervision target for Markovian scale prediction. Markov-VAR is trained under the teacher-forcing scheme while further adopting the Markovian attention shown in Figure 3, restricting each scale to attend only to its current state. Other main strategies remain consistent with standard visual autoregressive training.

Algorithm 1 shows the training process, where modules with subscript θ are learnable. \hat{f} denotes the final target feature of Markov-VAR. $\mathcal{F} = [\langle \text{sos} \rangle, X_1, \dots, X_{T-1}]$ represents a queue of token sequences. The overall scale sequence \hat{R} consist of the residual features predicted for each scale. Finally, the training loss \mathcal{L} is calculated by the cross-entropy (CE) [45] between the ground-truth R with \hat{R} .

4. Experiment

4.1. Experiment Settings

Models and Baselines. We construct Markov-VAR models with depths d of 16, 20, and 24 layers, the network structure is set as: the width $w = 64d$, the number of attention heads $h = d$ and the dropout rate $dr = 0.1 \cdot d/24$. We utilize Rotary Positional Embedding [49] for learnable positional encoding, and adopt LLaMA-style [55] attention and MLP blocks following [51]. For image tokenization,

we employ the pre-trained multi-scale VQ-VAE tokenizer from VAR. To evaluate the effectiveness of our design, we compare Markov-VAR with the VAR [52] and other VAR-like models on comparable model sizes. We further include comparisons with broad generative models of alternative paradigms, such as diffusion models, GANs, and next-token prediction autoregressive models, to provide a comprehensive evaluation.

Datasets and Metrics. We conduct the pre-training of Markov-VAR on the ImageNet-1K dataset [9], following the standard class-to-image generation model setting. For quantitative evaluation, we use Fréchet Inception Distance (FID), Inception Score (IS), Precision, and Recall as the primary metrics to comprehensively assess generation quality. We evaluate efficiency in terms of inference time and peak GPU memory consumption of computation state, which is mainly composed of Transformer activations and KV cache.

Implementation Details. All models are trained in similar settings, with a base learning rate of 8×10^{-5} , using the AdamW optimizer [33] with $\beta_1 = 0.9$ and $\beta_2 = 0.95$. The batch size ranges from 768 to 1536, and the training epochs vary from 200 to 400, depending on the model depth. Training is implemented on 8 NVIDIA H200 GPUs. Evaluation is conducted on a single NVIDIA H200 GPU.

Table 1. Performance comparison on ImageNet 256×256 class-conditional generation with VAR and VAR-like models. Evaluation metrics include Fréchet Inception Distance (FID) and Inception Score (IS). Precision and Recall jointly assess the fidelity–diversity trade-off of generated images. ‘↓’ and ‘↑’ indicate that lower or higher values are preferable.

Model	Param	FID↓	IS↑	Precision↑	Recall↑
M-VAR- <i>d20</i> [41]	900M	2.41	308.4	0.85	0.58
FlexVAR- <i>d24</i> [21]	1.0B	2.21	299.1	0.83	0.59
HMAR- <i>d24</i> [24]	1.3B	2.10	324.3	0.83	0.60
NestAR-H [63]	1.3B	2.22	342.4	0.79	0.57
VAR- <i>d16</i> [52]	310M	3.61	225.6	0.81	0.52
VAR- <i>d20</i> [52]	600M	2.67	254.4	0.81	0.57
VAR- <i>d24</i> [52]	1.0B	2.17	271.9	0.81	0.59
VAR- <i>d30</i> [52]	2.0B	2.14	275.4	0.80	0.60
Markov-VAR- <i>d16</i>	329.0M	3.23	256.2	0.84	0.52
Markov-VAR- <i>d20</i>	623.2M	2.44	286.1	0.83	0.56
Markov-VAR- <i>d24</i>	1.02B	2.15	310.9	0.83	0.59

4.2. Main Results

Generation Performance. We first evaluate the generation performance of Markov-VAR. We conduct comparison with VAR and other VAR-like models [17, 24, 41, 63] on ImageNet 256 × 256 class-conditional image generation. As shown in Table 1, Markov-VAR demonstrates a comprehensively better performance, achieving higher generation quality than other VAR models of comparable size.

Table 2. Board performance comparison on class-to-image generation on ImageNet 256×256 benchmark with more alternative-paradigm models. Step metric accounts for the number of sampling steps during inference. The suffix ‘-re’ denotes rejection sampling.

Type	Model	Parameter	FID↓	IS↑	Precision↑	Recall↑	Step
GAN	BigGAN [3]	112M	6.95	224.5	0.89	0.38	1
GAN	GigaGAN [22]	569M	3.45	225.5	0.84	0.61	1
GAN	StyleGAN-XL [44]	166M	2.30	265.1	0.78	0.53	1
Diffusion	ADM [10]	554M	10.94	101.0	0.69	0.63	250
Diffusion	CDM [20]	-	4.88	158.7	-	-	8100
Diffusion	LDM-4 [42]	400M	3.60	247.7	-	-	250
Diffusion	DiT-XL/2 [37]	675M	2.27	278.2	0.83	0.57	250
Masked AR	MaskGIT [4]	227M	6.18	182.1	0.80	0.51	8
Masked AR	MaskGIT-re [28]	227M	4.02	355.6	-	8	
Masked AR	MAGE [29]	230M	6.93	195.8	-	-	20
Next-token AR	VQGAN [13]	227M	18.65	80.4	0.78	0.26	256
Next-token AR	VQGAN [13]	1.4B	15.76	74.3	-	-	256
Next-token AR	VQGAN-re [68]	1.4B	5.20	280.3	-	-	256
Next-token AR	ViT-VQGAN [68]	1.7B	4.17	175.1	-	-	1024
Next-token AR	ViT-VQGAN-re [68]	1.7B	3.04	227.4	-	-	1024
Next-token AR	RQTran [25]	3.8B	7.55	80.4	0.78	0.26	68
Next-token AR	RQTran-re [25]	3.8B	3.80	323.7	-	-	68
Next-token AR	LlamaGen-B [50]	111M	5.46	193.6	0.83	0.45	256
Next-token AR	LlamaGen-L [50]	343M	3.81	248.3	0.83	0.52	256
Next-token AR	LlamaGen-XL [50]	775M	3.39	227.1	0.81	0.54	256
Next-token AR	LlamaGen-XXL [50]	1.4B	3.09	253.6	0.83	0.53	256
Markovian Scale AR	Markov-VAR- <i>d16</i>	329.0M	3.23	256.2	0.84	0.52	10
Markovian Scale AR	Markov-VAR- <i>d20</i>	623.2M	2.44	286.1	0.83	0.56	10
Markovian Scale AR	Markov-VAR- <i>d24</i>	1.02B	2.15	310.9	0.83	0.59	10

For example, on the *depth-16* model, Markov-VAR improve the FID performance from 3.61 to 3.23 (10.5%) and IS performance from 225.6 to 256.2 (13.6%) compared to VAR. Even on Precision and Recall metrics, Markov-VAR matches or surpasses VAR. Markov-VAR’s advantages can be observed across other sizes. Compared with M-VAR-*d20*, Markov-VAR-*d20* achieves compelling performance while using only 70% of its parameters, demonstrating that Markov-VAR is both effective and parameter-efficient.

To further demonstrate the performance advancements of Markov-VAR. We conduct a board comparison on class-to-image generation on ImageNet 256×256 benchmark with more alternative-paradigm models, including GANs [3, 22, 44], diffusion models [10, 19, 37, 42], mask autoregressive models [4, 28, 29], and next-token prediction autoregressive models [13, 25, 50, 68]. As shown in Table 2, Compared with Diffusion models, Markov-VAR achieves better overall performance in terms of both parameter efficiency and generation quality. Compared to the size-similar next-token autoregressive model LlamaGen-L, Markov-VAR achieves superior performance across all evaluation metrics. In contrast to other autoregressive models, Markov-VAR maintains competitive generation quality while requiring fewer sampling steps, demonstrating its higher inference efficiency. Further comparisons in the ta-

ble also reveal Markov-VAR’s favorable generation performance and parameter efficiency.

Generation Efficiency. We also evaluate the computational efficiency of Markov-VAR with various resolutions and depths compared to VAR [52] and other VAR-like models [21, 24]. As shown in Table 3, Markov-VAR achieve consistently excellent performance on efficiency metrics. For peak memory consumption, at 256×256 , Markov-VAR-*d16* reduces it by 56.9%, and Markov-VAR-*d24* reduces it by 62.1%. As resolution increases, the memory advantage becomes increasingly evident: Markov-VAR-*d24* brings peak memory consumption down from 117.9GB to 19.1GB (83.8%) at 1024×1024 . Moreover, compared to the other VAR-like model FlexVAR, Markov-VAR achieves an acceleration of $1.33\times$ for inference at 256×256 . These results demonstrate the efficiency of Markov-VAR.

4.3. Ablation and Analysis

Ablation on History Compensation Mechanism. To verify the effectiveness of our sliding-window-based history compensation mechanism, we conduct ablation and further compare ours to other mechanisms. Global history is a full-context compensation, which continuously fuses and updates all previous scales, and hybrid history combines both

Table 3. Comparison of inference time and peak memory between Markov-VAR and other VAR-like models across various resolutions and depths. Peak GPU memory is reported as the average of 5 runs with a batch size of 25 on a single NVIDIA H200. Inference time is measured in seconds per batch on a NVIDIA H200.

Model	Depth	Res.	Time(s) ↓	Memory(GB) ↓
VAR [52]	16	256	0.303	5.8
VAR [52]	16	512	0.824	18.4
VAR [52]	16	1024	3.303	66.7
HMAR [24]	16	256	0.309	3.1
HMAR [24]	16	512	0.909	5.6
FlexVAR [21]	16	256	0.395	6.8
FlexVAR [21]	16	512	0.944	20.1
FlexVAR [21]	16	1024	3.409	77.9
Markov-VAR	16	256	0.296	2.5
Markov-VAR	16	512	0.780	4.9
Markov-VAR	16	1024	3.125	14.6
VAR [52]	24	256	0.711	12.4
VAR [52]	24	512	1.335	31.4
VAR [52]	24	1024	5.891	117.9
Markov-VAR	24	256	0.608	4.7
Markov-VAR	24	512	1.261	8.1
Markov-VAR	24	1024	5.322	19.1

full-context and non-full-context compensation. In Table 4, all types of compensation mechanism improve generation quality compared to the one without history compensation. However, our sliding-window-based history compensation mechanism achieves the overall best preservation of historical information. These validate the effectiveness of our design and are consistent with the analysis in Section 3.3.

Table 4. History compensation ablation on the depth-16 model across different history compensation mechanisms.

Method	Depth	Param	FID ↓	IS ↑
w/o History	16	300M	3.64	247.7
Global History	16	324M	3.41	245.2
Hybrid History	16	359M	3.45	257.4
Ours	16	329M	3.23	256.2

Ablation on Sliding Window Size. To determine a suitable sliding window size for Markov-VAR’s history compensation mechanism, we conduct an ablation study on Markov-VAR with depths of 16 and 20. As shown in Table 5, models with the two depths consistently achieve their best performance when window size is set to 3. In comparison, when the window size is set to 1, Markov-VAR-*d16* respectively decreases FID and IS to 3.53 and 237.8. All these results are also consistent with the analysis of cross-scale interference discussed in Introduction that full-context dependency may hinders distinctive scale feature learning, and the most recent three scales typically have a positive effect on learning.

Table 5. Ablation study of the sliding-window-based history compensation mechanism with different window sizes.

Window Size	FID(d16) ↓	IS(d16) ↑	FID(d20) ↓	IS(d20) ↑
1	3.53	237.8	2.50	267.9
2	3.39	248.6	2.47	281.4
3	3.23	256.2	2.44	286.1
4	3.33	252.3	2.56	278.2

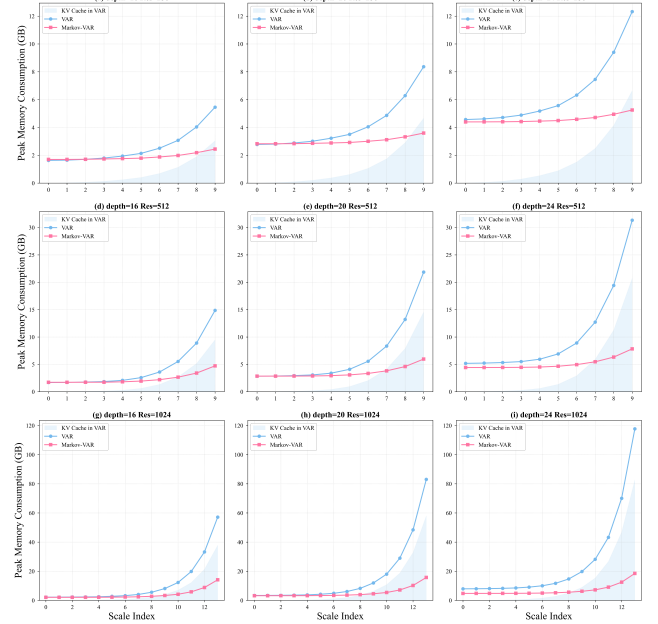


Figure 4. Analysis of peak memory consumption of Markov-VAR across various depths and resolutions at different scales.

Memory Consumption Analysis. As shown in Figure 4, we investigated the peak memory consumption of computation state across various depths and resolutions at different scales. Compared with VAR, Markov-VAR exhibits a less steep scaling trend rather than the exponential growth trend observed in VAR. As the model size and target resolution increase, the efficiency advantage of Markov-VAR becomes increasingly evident. Most importantly, because Markov-VAR follows a Markovian modeling process, it does not require any KV-cache computation, which fundamentally accounts for its significantly lower computational cost. Moreover, even the computation of Transformer activation in VAR is also larger than that of Markov-VAR, further demonstrating the computational efficiency advantage of Markov-VAR. All these results demonstrate that Markovian Scale Prediction effectively alleviates the exponential growth of full-context modeling, making it more promising for scaling and generating visual content at larger scales.

Analysis of Scaling Law. We vary the depth of Markov-VAR from 6 to 24 to analyze the scaling law, correspond-

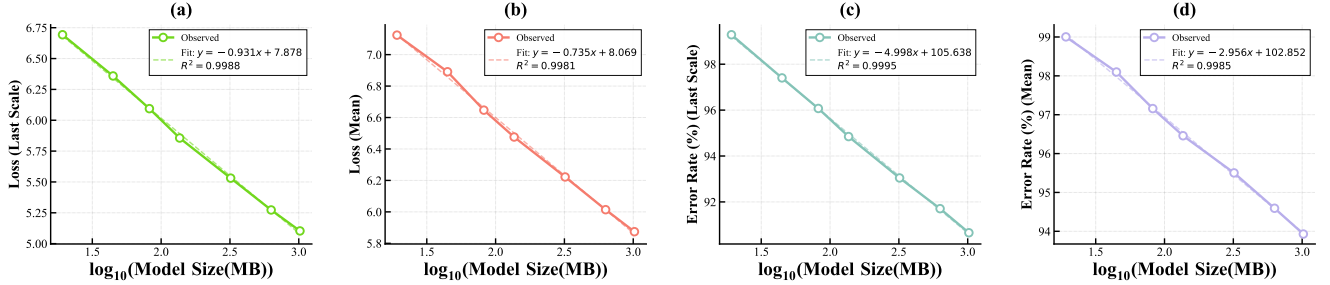


Figure 5. Scaling law analysis of Markov-VAR between performance metrics and model sizes with power-law fitted equations.



Figure 6. Visualization of generation process in Markov-VAR at 256×256 resolution.

ing to parameter scales ranging from 19.80M to 1.02B. As shown in Figure 5, charts (a) to (d) show the fitted scaling relation between model size (\log_{10}) and performance metrics. Both loss and error rate consistently decrease as model size increases, following obvious power-law trends with high coefficients of determination ($R^2 > 0.99$), indicating that Markov-VAR preliminarily follows the expected scaling law on model size.

4.4. Visualization

Main Generation Visualization. Figure 1 shows representative image samples generated by our Markov-VAR. Given the scale and quality of ImageNet, Markov-VAR performs reasonably well. Its generation quality may further improve when trained on larger and higher-quality datasets.

Visualization of Generation Process We visualize the Markovian scale prediction process in Figure 6. This visualization provides an intuitive understanding of how Markov-VAR constructs a semantic structure and fills in fine-grained details across multiple scales. The earliest scales capture only very coarse global structures, such as rough color distributions and object silhouettes. As the scale increases, the model gradually refines the semantics. Later scales enrich high-frequency textures and refine local details such as fur patterns and cloud shapes. Notably, the refinement is both smooth and consistent, demonstrating that each Markovian scale effectively preserves essential historical information without relying on full-context dependency.

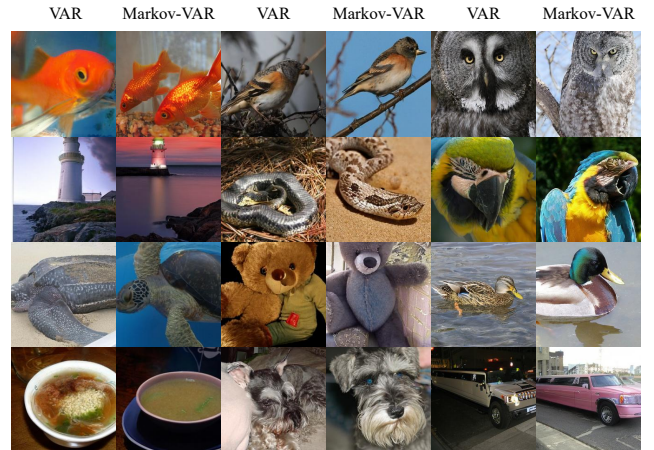


Figure 7. Visual comparison between VAR and Markov-VAR.

Visual Comparison between VAR and Markov-VAR. Figure 7 shows that both models perform well on certain generated samples, even in some cases, Markov-VAR even produces better semantics and higher quality than VAR.

5. Conclusion

In this paper, we address the challenges of VAR’s full-context dependency by reformulating it as a Markov process. We propose Markov-VAR, which employs Markovian scale prediction by treating each scale as a Markov state and modeling its evolution as a Markov process. Experiments and analysis demonstrate that Markov-VAR achieves effective and efficient visual generation.

References

- [1] Josh Achiam, Steven Adler, Sandhini Agarwal, Lama Ahmad, Ilge Akkaya, Florencia Leoni Aleman, Diogo Almeida, Janko Altenschmidt, Sam Altman, Shyamal Anadkat, et al. Gpt-4 technical report. *arXiv preprint arXiv:2303.08774*, 2023. 2
- [2] Alexander A. Alemi, Ian Fischer, Joshua V. Dillon, and Kevin Murphy. Deep variational information bottleneck, 2019. 2, 4
- [3] Andrew Brock, Jeff Donahue, and Karen Simonyan. Large scale gan training for high fidelity natural image synthesis. *arXiv preprint arXiv:1809.11096*, 2018. 6
- [4] Huiwen Chang, Han Zhang, Lu Jiang, Ce Liu, and William T Freeman. Maskgit: Masked generative image transformer. In *Proceedings of the IEEE/CVF conference on computer vision and pattern recognition*, pages 11315–11325, 2022. 6
- [5] Yongwei Chen, Yushi Lan, Shangchen Zhou, Tengfei Wang, and Xingang Pan. Sar3d: Autoregressive 3d object generation and understanding via multi-scale 3d vqvae. In *Proceedings of the Computer Vision and Pattern Recognition Conference*, pages 28371–28382, 2025. 3
- [6] Zhe Chen, Jiannan Wu, Wenhai Wang, Weijie Su, Guo Chen, Sen Xing, Muyan Zhong, Qinglong Zhang, Xizhou Zhu, Lewei Lu, Bin Li, Ping Luo, Tong Lu, Yu Qiao, and Jifeng Dai. Internvl: Scaling up vision foundation models and aligning for generic visual-linguistic tasks. In *Proceedings of the IEEE/CVF Conference on Computer Vision and Pattern Recognition (CVPR)*, pages 24185–24198, 2024. 2
- [7] Hyung Won Chung, Le Hou, Shayne Longpre, Barret Zoph, Yi Tay, William Fedus, Yunxuan Li, Xuezhi Wang, Mostafa Dehghani, Siddhartha Brahma, et al. Scaling instruction-finetuned language models. *Journal of Machine Learning Research*, 25(70):1–53, 2024. 2
- [8] Florinel-Alin Croitoru, Vlad Hondru, Radu Tudor Ionescu, and Mubarak Shah. Diffusion models in vision: A survey. *IEEE transactions on pattern analysis and machine intelligence*, 45(9):10850–10869, 2023. 3
- [9] Jia Deng, Wei Dong, Richard Socher, Li-Jia Li, Kai Li, and Li Fei-Fei. Imagenet: A large-scale hierarchical image database. In *2009 IEEE conference on computer vision and pattern recognition*, pages 248–255. Ieee, 2009. 3, 5
- [10] Prafulla Dhariwal and Alexander Nichol. Diffusion models beat gans on image synthesis. *Advances in neural information processing systems*, 34:8780–8794, 2021. 6
- [11] Ming Ding, Zhuoyi Yang, Wenyi Hong, Wendi Zheng, Chang Zhou, Da Yin, Junyang Lin, Xu Zou, Zhou Shao, Hongxia Yang, and Jie Tang. Cogview: Mastering text-to-image generation via transformers, 2021. 3
- [12] Patrick Esser, Robin Rombach, Andreas Blattmann, and Bjorn Ommer. Imagebart: Bidirectional context with multinomial diffusion for autoregressive image synthesis. *Advances in neural information processing systems*, 34:3518–3532, 2021. 3
- [13] Patrick Esser, Robin Rombach, and Bjorn Ommer. Taming transformers for high-resolution image synthesis. In *Proceedings of the IEEE/CVF conference on computer vision and pattern recognition*, pages 12873–12883, 2021. 6
- [14] Ian J Goodfellow, Jean Pouget-Abadie, Mehdi Mirza, Bing Xu, David Warde-Farley, Sherjil Ozair, Aaron Courville, and Yoshua Bengio. Generative adversarial nets. *Advances in neural information processing systems*, 27, 2014. 3
- [15] Hang Guo, Yawei Li, Taolin Zhang, Jiangshan Wang, Tao Dai, Shu-Tao Xia, and Luca Benini. Fastvar: Linear visual autoregressive modeling via cached token pruning. *arXiv preprint arXiv:2503.23367*, 2025. 3
- [16] Xun Guo, Mingwu Zheng, Liang Hou, Yuan Gao, Yufan Deng, Pengfei Wan, Di Zhang, Yufan Liu, Weiming Hu, Zhengjun Zha, et al. I2v-adapter: A general image-to-video adapter for diffusion models. In *ACM SIGGRAPH 2024 Conference Papers*, pages 1–12, 2024. 3
- [17] Jian Han, Jinlai Liu, Yi Jiang, Bin Yan, Yuqi Zhang, Zehuan Yuan, Bingyue Peng, and Xiaobing Liu. Infinity: Scaling bit-wise autoregressive modeling for high-resolution image synthesis. In *Proceedings of the Computer Vision and Pattern Recognition Conference*, pages 15733–15744, 2025. 2, 3, 5
- [18] Jonathan Ho, Ajay Jain, and Pieter Abbeel. Denoising diffusion probabilistic models. *Advances in neural information processing systems*, 33:6840–6851, 2020. 3
- [19] Jonathan Ho, Ajay Jain, and Pieter Abbeel. Denoising diffusion probabilistic models. *Advances in neural information processing systems*, 33:6840–6851, 2020. 3, 6
- [20] Jonathan Ho, Chitwan Saharia, William Chan, David J Fleet, Mohammad Norouzi, and Tim Salimans. Cascaded diffusion models for high fidelity image generation. *Journal of Machine Learning Research*, 23(47):1–33, 2022. 6
- [21] Siyu Jiao, Gengwei Zhang, Yinlong Qian, Jiancheng Huang, Yao Zhao, Humphrey Shi, Lin Ma, Yunchao Wei, and Zequn Jie. Flexvar: Flexible visual autoregressive modeling without residual prediction. *arXiv preprint arXiv:2502.20313*, 2025. 3, 5, 6, 7
- [22] Minguk Kang, Jun-Yan Zhu, Richard Zhang, Jaesik Park, Eli Shechtman, Sylvain Paris, and Taesung Park. Scaling up gans for text-to-image synthesis. In *Proceedings of the IEEE/CVF conference on computer vision and pattern recognition*, pages 10124–10134, 2023. 6
- [23] Nupur Kumari, Bingliang Zhang, Richard Zhang, Eli Shechtman, and Jun-Yan Zhu. Multi-concept customization of text-to-image diffusion. In *Proceedings of the IEEE/CVF conference on computer vision and pattern recognition*, pages 1931–1941, 2023. 3
- [24] Hermann Kumbong, Xian Liu, Tsung-Yi Lin, Ming-Yu Liu, Xihui Liu, Ziwei Liu, Daniel Y Fu, Christopher Re, and David W Romero. Hmar: Efficient hierarchical masked autoregressive image generation. In *Proceedings of the Computer Vision and Pattern Recognition Conference*, pages 2535–2544, 2025. 2, 3, 5, 6, 7
- [25] Doyup Lee, Chiheon Kim, Saehoon Kim, Minsu Cho, and Wook-Shin Han. Autoregressive image generation using residual quantization. In *Proceedings of the IEEE/CVF Conference on Computer Vision and Pattern Recognition*, pages 11523–11532, 2022. 6
- [26] Doyup Lee, Chiheon Kim, Saehoon Kim, Minsu Cho, and Wook-Shin Han. Autoregressive image generation using residual quantization. In *Proceedings of the IEEE/CVF con-*

- ference on computer vision and pattern recognition*, pages 11523–11532, 2022. 3
- [27] Feng Li, Renrui Zhang, Hao Zhang, Yuanhan Zhang, Bo Li, Wei Li, Zejun Ma, and Chunyuan Li. Llava-next-interleave: Tackling multi-image, video, and 3d in large multimodal models. *arXiv preprint arXiv:2407.07895*, 2024. 2
- [28] Tianhong Li, Huiwen Chang, Shlok Mishra, Han Zhang, Dina Katabi, and Dilip Krishnan. Mage: Masked generative encoder to unify representation learning and image synthesis. In *Proceedings of the IEEE/CVF Conference on Computer Vision and Pattern Recognition*, pages 2142–2152, 2023. 6
- [29] Tianhong Li, Yonglong Tian, He Li, Mingyang Deng, and Kaiming He. Autoregressive image generation without vector quantization, 2024. 6
- [30] Xiang Li, Kai Qiu, Hao Chen, Jason Kuen, Zhe Lin, Rita Singh, and Bhiksha Raj. Controlvar: Exploring controllable visual autoregressive modeling. *arXiv preprint arXiv:2406.09750*, 2024. 3
- [31] Jinlai Liu, Jian Han, Bin Yan, Hui Wu, Fengda Zhu, Xing Wang, Yi Jiang, Bingyue Peng, and Zehuan Yuan. Infinitystar: Unified spacetime autoregressive modeling for visual generation, 2025. 3
- [32] Jiayu Liu, Zhenya Huang, Anya Sims, Enhong Chen, Yee Whye Teh, and Ning Miao. Marcos: Deep thinking by markov chain of continuous thoughts. *arXiv preprint arXiv:2509.25020*, 2025. 3
- [33] Ilya Loshchilov and Frank Hutter. Decoupled weight decay regularization. *arXiv preprint arXiv:1711.05101*, 2017. 5
- [34] Weichao Mao, Kaiqing Zhang, Erik Miehl, and Tamer Başar. Information state embedding in partially observable cooperative multi-agent reinforcement learning. In *2020 59th IEEE Conference on Decision and Control (CDC)*, pages 6124–6131. IEEE, 2020. 3
- [35] Andrei Andreevich Markov. Rasprostranenie zakona bol'shih chisel na velichiny, zavisyaschie drug ot druga. *Izvestiya Fiziko-matematicheskogo obschestva pri Kazanskom universitete*, 15(135-156):18, 1906. 3
- [36] Shen Nie, Fengqi Zhu, Zebin You, Xiaolu Zhang, Jingyang Ou, Jun Hu, Jun Zhou, Yankai Lin, Ji-Rong Wen, and Chongxuan Li. Large language diffusion models. *arXiv preprint arXiv:2502.09992*, 2025. 3
- [37] William Peebles and Saining Xie. Scalable diffusion models with transformers. In *Proceedings of the IEEE/CVF international conference on computer vision*, pages 4195–4205, 2023. 6
- [38] Yunpeng Qu, Kun Yuan, Jinhua Hao, Kai Zhao, Qizhi Xie, Ming Sun, and Chao Zhou. Visual autoregressive modeling for image super-resolution. *arXiv preprint arXiv:2501.18993*, 2025. 3
- [39] Sudarshan Rajagopalan, Kartik Narayan, and Vishal M Patel. Restorevar: Visual autoregressive generation for all-in-one image restoration. *arXiv preprint arXiv:2505.18047*, 2025. 3
- [40] Aditya Ramesh, Mikhail Pavlov, Gabriel Goh, Scott Gray, Chelsea Voss, Alec Radford, Mark Chen, and Ilya Sutskever. Zero-shot text-to-image generation. In *International conference on machine learning*, pages 8821–8831. Pmlr, 2021. 3
- [41] Sucheng Ren, Yaodong Yu, Nataniel Ruiz, Feng Wang, Alan Yuille, and Cihang Xie. M-var: Decoupled scale-wise autoregressive modeling for high-quality image generation. 2024. 2, 5
- [42] Robin Rombach, Andreas Blattmann, Dominik Lorenz, Patrick Esser, and Björn Ommer. High-resolution image synthesis with latent diffusion models. In *Proceedings of the IEEE/CVF conference on computer vision and pattern recognition*, pages 10684–10695, 2022. 6
- [43] Tim Salimans, Andrej Karpathy, Xi Chen, and Diederik P Kingma. Pixelcnn++: Improving the pixelcnn with discretized logistic mixture likelihood and other modifications. *arXiv preprint arXiv:1701.05517*, 2017. 3
- [44] Axel Sauer, Katja Schwarz, and Andreas Geiger. Stylegan-xl: Scaling stylegan to large diverse datasets. In *ACM SIGGRAPH 2022 conference proceedings*, pages 1–10, 2022. 6
- [45] Claude E Shannon. A mathematical theory of communication. *The Bell system technical journal*, 27(3):379–423, 1948. 5
- [46] Chenze Shao, Fandong Meng, and Jie Zhou. Continuous visual autoregressive generation via score maximization. *arXiv preprint arXiv:2505.07812*, 2025. 2
- [47] Hui Shen, Jingxuan Zhang, Boning Xiong, Rui Hu, Shoufa Chen, Zhongwei Wan, Xin Wang, Yu Zhang, Zixuan Gong, Guangyin Bao, et al. Efficient diffusion models: A survey. *arXiv preprint arXiv:2502.06805*, 2025. 3
- [48] Jiaming Song, Chenlin Meng, and Stefano Ermon. Denoising diffusion implicit models. *arXiv preprint arXiv:2010.02502*, 2020. 3
- [49] Jianlin Su, Yu Lu, Shengfeng Pan, Ahmed Murtadha, Bo Wen, and Yunfeng Liu. Roformer: Enhanced transformer with rotary position embedding, 2023. 5
- [50] Peize Sun, Yi Jiang, Shoufa Chen, Shilong Zhang, Bingyue Peng, Ping Luo, and Zehuan Yuan. Autoregressive model beats diffusion: Llama for scalable image generation. *arXiv preprint arXiv:2406.06525*, 2024. 6
- [51] Haotian Tang, Yecheng Wu, Shang Yang, Enze Xie, Junsong Chen, Junyu Chen, Zhuoyang Zhang, Han Cai, Yao Lu, and Song Han. Hart: Efficient visual generation with hybrid autoregressive transformer. *arXiv preprint arXiv:2410.10812*, 2024. 3, 5
- [52] Keyu Tian, Yi Jiang, Zehuan Yuan, Bingyue Peng, and Liwei Wang. Visual autoregressive modeling: Scalable image generation via next-scale prediction. *Advances in neural information processing systems*, 37:84839–84865, 2024. 2, 3, 5, 6, 7
- [53] Naftali Tishby and Noga Zaslavsky. Deep learning and the information bottleneck principle. In *2015 IEEE Information Theory Workshop (ITW)*, pages 1–5, 2015. 2, 4
- [54] Naftali Tishby, Fernando C. Pereira, and William Bialek. The information bottleneck method, 2000. 2, 4
- [55] Hugo Touvron, Thibaut Lavril, Gautier Izacard, Xavier Martinet, Marie-Anne Lachaux, Timothée Lacroix, Baptiste Rozière, Naman Goyal, Eric Hambro, Faisal Azhar, et al. Llama: Open and efficient foundation language models. *arXiv preprint arXiv:2302.13971*, 2023. 2, 5

- [56] Aaron Van den Oord, Nal Kalchbrenner, Lasse Espeholt, Oriol Vinyals, Alex Graves, et al. Conditional image generation with pixelcnn decoders. *Advances in neural information processing systems*, 29, 2016. 3
- [57] Aäron Van Den Oord, Nal Kalchbrenner, and Koray Kavukcuoglu. Pixel recurrent neural networks. In *International conference on machine learning*, pages 1747–1756. PMLR, 2016. 3
- [58] Aaron Van Den Oord, Oriol Vinyals, et al. Neural discrete representation learning. *Advances in neural information processing systems*, 30, 2017. 3
- [59] Zhongwei Wan, Xin Wang, Che Liu, Samiul Alam, Yu Zheng, Jiachen Liu, Zhongnan Qu, Shen Yan, Yi Zhu, Quanlu Zhang, et al. Efficient large language models: A survey. *arXiv preprint arXiv:2312.03863*, 2023. 2
- [60] Zhongwei Wan, Xinjian Wu, Yu Zhang, Yi Xin, Chaofan Tao, Zhihong Zhu, Xin Wang, Siqi Luo, Jing Xiong, and Mi Zhang. D2o: Dynamic discriminative operations for efficient generative inference of large language models. *arXiv preprint arXiv:2406.13035*, 2024. 2
- [61] Yufei Wang, Lanqing Guo, Zhihao Li, Jiaxing Huang, Pichao Wang, Bihan Wen, and Jian Wang. Training-free text-guided image editing with visual autoregressive model. *arXiv preprint arXiv:2503.23897*, 2025. 3
- [62] Eric Wiewiora. Learning predictive representations from a history. In *Proceedings of the 22nd international conference on Machine learning*, pages 964–971, 2005. 3
- [63] Hongyu Wu, Xuhui Fan, Zhangkai Wu, and Longbing Cao. Nested autoregressive models, 2025. 3, 5
- [64] Jiye Xie, Yifei Gao, Liangliang You, Xiang Xu, Haoran Xu, Zhiqiang Kou, Kexue Fu, Youyang Qu, Wenjie Yang, Jianwei Guo, et al. Collaboration wins more: Dual-modal collaborative attention reinforcement for mitigating large vision language models hallucination. In *Proceedings of the 33rd ACM International Conference on Multimedia*, pages 4137–4146, 2025. 2
- [65] Rui Xie, Tianchen Zhao, Zhihang Yuan, Rui Wan, Wenxi Gao, Zhenhua Zhu, Xuefei Ning, and Yu Wang. Litevar: Compressing visual autoregressive modelling with efficient attention and quantization. *arXiv preprint arXiv:2411.17178*, 2024. 3
- [66] Lujie Yang, Kaiqing Zhang, Alexandre Amice, Yunzhu Li, and Russ Tedrake. Discrete approximate information states in partially observable environments. In *2022 American Control Conference (ACC)*, pages 1406–1413. IEEE, 2022. 3
- [67] Wen Yang, Minpeng Liao, and Kai Fan. Markov chain of thought for efficient mathematical reasoning. *arXiv preprint arXiv:2410.17635*, 2024. 3
- [68] Jiahui Yu, Xin Li, Jing Yu Koh, Han Zhang, Ruoming Pang, James Qin, Alexander Ku, Yuanzhong Xu, Jason Baldridge, and Yonghui Wu. Vector-quantized image modeling with improved vqgan. *arXiv preprint arXiv:2110.04627*, 2021. 6
- [69] Jiahui Yu, Yuanzhong Xu, Jing Yu Koh, Thang Luong, Gunjan Baid, Zirui Wang, Vijay Vasudevan, Alexander Ku, Yinfei Yang, Burcu Karagol Ayan, Ben Hutchinson, Wei Han, Zarana Parekh, Xin Li, Han Zhang, Jason Baldridge, and Yonghui Wu. Scaling autoregressive models for content-rich text-to-image generation, 2022. 3
- [70] Qian Zhang, Xiangzi Dai, Ninghua Yang, Xiang An, Ziyong Feng, and Xingyu Ren. Var-clip: Text-to-image generator with visual auto-regressive modeling. *arXiv preprint arXiv:2408.01181*, 2024. 3
- [71] Yu Zhang, Jialei Zhou, Xinchun Li, Qi Zhang, Zhongwei Wan, Duoqian Miao, Changwei Wang, and Longbing Cao. Enhancing text-to-image diffusion transformer via split-text conditioning. In *The Thirty-ninth Annual Conference on Neural Information Processing Systems*. 3
- [72] Fengqi Zhu, Rongzhen Wang, Shen Nie, Xiaolu Zhang, Chunwei Wu, Jun Hu, Jun Zhou, Jianfei Chen, Yankai Lin, Ji-Rong Wen, et al. Llada 1.5: Variance-reduced preference optimization for large language diffusion models. *arXiv preprint arXiv:2505.19223*, 2025. 3
- [73] Lei Zhu, Fangyun Wei, Yanye Lu, and Dong Chen. Scaling the codebook size of vq-gan to 100,000 with a utilization rate of 99%. *Advances in Neural Information Processing Systems*, 37:12612–12635, 2024. 3
- [74] Xianwei Zhuang, Yuxin Xie, Yufan Deng, Dongchao Yang, Liming Liang, Jinghan Ru, Yuguo Yin, and Yuexian Zou. Vargpt-v1. 1: Improve visual autoregressive large unified model via iterative instruction tuning and reinforcement learning. *arXiv preprint arXiv:2504.02949*, 2025. 3